DSPACE

https://dspace.org/

Failure analysis of geothermal API 5L grade Bsteel pipeline

J Obiko; M Ndeto; J Mutua; B Shongwe; N Malatji ...

https://hdl.handle.net/10539/46785
SCOPUS

Downloaded from a DSpace repository. https://dspace.org/

Engineering Solid Mechanics 13 (2025) 259-266

Contents lists available at GrowingScience

Engineering Solid Mechanics

homepage: www.GrowingScience.com/esm

Failure analysis of geothermal API 5L grade B steel pipeline

J. Obiko[a*], M. Ndeto[b], J. Mutua[b], B. Shongwe[a], N. Malatji[a], M. Bodunrin[c] and D. Klenam[c]

[a]*Tshwane University of Technology, Department of Chemical, Metallurgical, and Materials Engineering, Pretoria, South Africa*
[b]*Jomo Kenyatta University of Agriculture and Technology, Department of Mechanical Engineering, Nairobi, Kenya*
[c]*University of the Witwatersrand, School of Chemical and Metallurgical Engineering, Johannesburg, 2000, South Africa*

ARTICLE INFO

Article history:
Received 22 January 2025
Accepted 4 May 2025
Available online
4 May 2025

Keywords:
Geothermal
Steam pipeline
Failure mechanism
Erosion-corrosion

ABSTRACT

This article reports on the failure analysis of the geothermal steam pipe. Macro and micro examination of failed pipelines was studied using optical and scanning electron microscopy. The energy-dispersive spectroscopy studied the elemental composition of the corroded surface. Further, the study measured the pipe thickness on the failed pipeline section. Visual examination showed a significant thinning of the outer section of the failed pipe to 3 mm from 12.7 mm of the original pipe. The chemical composition results show that the steel meets the minimum requirements for API 5L Grade B steels used in steam pipelines for geothermal power plants. The microstructural analysis of the investigated steel shows that the steel had pearlite and ferrite phases. The steel failure mechanism was due to erosion-corrosion, which caused localised wall thinning near the drain port and elbow section. The study recommends creep-resistant steel for the drain port and elbow for geothermal power plant application.

© 2025 Growing Science Ltd. All rights reserved.

1. Introduction

Industrial development and population growth have caused electricity demand (Carbos et al., 2020; Sharma & Maheshwari, 2017). Globally, there is a shift from fossil-fuel power plants to green energy, such as geothermal power plants, due to stringent environmental restrictions (Kusmono & Khasani, 2017). There is consensus on the reduction of CO_2 emission (Ávila et al., 2023). To ensure high thermal efficiency and reduction in CO_2 emissions, the design of new alloys has gained attention, especially for steam pipelines (Hu et al., 2022). These alloys should exhibit superior properties to operate in severe conditions (Ávila et al., 2023; Carbos et al., 2020; Ribeiro et al., 2021). For example, high-strength low-alloy steels such as X80 and X100 have a wide application for steam pipeline systems (Brownlie et al., 2021; Hu et al., 2022). These steels exhibit excellent strength and corrosion resistance (Liu et al., 2023). A study by Kusmono and Khasani (2017) shows that steam from geothermal wells contains corrosive agents such as CO_2, ammonia (NH_3), chloride and sulphate and hydrogen sulphide (H_2S). The pipeline system for transporting geothermal steam experiences a corrosive agent effect (Brownlie et al., 2021; Kusmono & Khasani, 2017). Therefore, a constant power supply requires a functioning steam pipeline. This aspect is critical to the designers and engineers during the manufacturing process. Failure of one component within the geothermal power plant causes a complete power plant shutdown. Most steam pipelines in geothermal power plants are of HSLA steel. An investigation and analysis to determine the cause of the steam pipeline failure is paramount to prevent catastrophic failure. Failure mechanisms identification is crucial in improving component integrity. Most steam pipelines fail due to corrosion, fatigue, erosion-corrosion and creep (Brownlie et al., 2021; Kusmono & Khasani, 2017; Wang et al., 2017). The failed steam pipe was API 5L Grade B X80 steel. The operating conditions were steam pressure (10 bar) and temperature (151°C), as shown in Table 2. The steam pipe failed after only ~ 52,000 hours in service due to the thinning of the outer wall of the steam pipe, causing catastrophic failure. The outer wall thickness was reduced from 12.7 mm to 3mm. This study investigated and analysed the failed steam pipe. The aim was to provide insights into the causes and mechanisms that accelerated pipeline

* Corresponding author.
E-mail addresses: japheth.obiko97@gmail.com (J. Obiko)

ISSN 2291-8752 (Online) - ISSN 2291-8744 (Print)
© 2025 Growing Science Ltd. All rights reserved.
doi: 10.5267/j.esm.2025.5.001

failure. Hence, propose the mitigation techniques. The study further reports on the prevention measures for future industrial design.

2. Experimental procedure

The study investigated a failed geothermal steam pipeline section. The optical emission spectrometer analysis determined the elemental chemical composition of the steam pipeline steel. The scanning electron microscopy (SEM/EDX) analysis also provided the chemical elements of the corroded steam pipeline surface. The metallography sample was ground and polished following the standard metallographic procedures. The study used 4% Nital solution to etch polished samples for microscopy analysis. The optical and scanning electron microscope analysed the steam pipeline microstructure.

3. Results and discussion

3.1. Macro-examination analysis

Fig. 1 shows photo images of different positions of geothermal steam pipeline failed sections. The extent and nature of the rupture indicate a catastrophic failure. Visual inspection revealed a significantly localised wall thinning of the pipeline. The pipe wall thickness measurement on the failed pipe was 3 mm, far less than the 12.7 mm measured for the upper side of the uncorroded pipe section. The failed steam pipeline had scales on the internal and external surfaces (**Fig. 1**). The steam pipeline failed after six years of operation. The cause of failure was due to high corrosion rates resulting from service conditions. The steam pipe thinning occurred over a period due to corrosion occurring near the drain port. The variation of steam temperature and pressure resulted in circumferentially pipe failure.

The failure cause was determined by sectioning the failed pipe section in as-received condition for microstructure characterisation. After six years of service, the analysis revealed that erosion corrosion caused the steam pipe to undergo severe thinner at sections near the drain port and in the bend, as illustrated in **Fig. 2**. The steam pipe scaling particles were present in the collected geothermal fluid. The scaling in the pipes appeared loose and porous. Regions that experienced turbulent and low-angle impeachment of steam flow had no scales adhered to the metal surfaces. The reason is that the scales fell off over time due to high service pressure as the material decomposed from the parent steel pipeline. The results further indicate that active erosion-corrosion is a cause of pipeline failure.

3.2. Chemical analysis

Table 1 shows the chemical composition of the failed pipe from two different chemical testing laboratories. From the chemical composition results, the steam pipe belongs to high strength low alloy (HSLA) steels (Villalobos et al., 2018). Table 2 shows detailed service conditions for geothermal plant material and steam properties.

Table 1. Chemical composition of investigated failed pipe.

Element	C	Mn	S	Si	Cu	Mo	Nb	V	Ti	Al	Cr	Ni	P	Co	Fe
Lab 1	0.119	0.63	0.008	0.16	0.03	≤0.01	≤0.005	≤0.005	≤0.005	0.03	0.02	0.02	0.021	0.006	Bal.
Lab 2	0.125	0.665	0.0074	0.203	0.0237	0.0046	0.004	0.004	0.0011	0.0325	0.0257	0.0145	0.0146	0.0029	Bal.

Table 2. Material specification and service conditions.

Material specification	**Material Grade**	**Carbon Steel API 5LGrB**
	Pipe diameter	DN1050
	Pipe thickness	12.7 mm
	Design service hours	30 years (262,800 Hours)
	Specifications for operating conditions	Line operating pressure is 10 Bars. Tested pressure was 13 Bars.
	Total hours of operation before failure	Approximately 52,713.18 hrs
	Low point drains dimensions	19.05 mm
Steam properties	Temperature	151°C
	Pressure	5 barg
	Dryness fraction	99.999% of steam
	Mass flow rate	265.75 tons for each pipe
	Steam Purity and Quality design specification	Upstream of the scrubber is < 1 mg/kg for sodium, iron and chloride, < 0.5 mg/kg for silica and < 5 mg/kg for TDS.



Fig. 1. Photographs of failed geothermal steam pipeline failure. (a) Ruptured pipe from original construction; (b) Repaired pipe around a drain port; (c) Repaired pipe around a bend; (d) & (e) Scaling and corrosion in pipes.

3.3. Microstructure analysis

Fig. 3 shows the optical image micrograph of the pipe investigated in this study. The image shows that the microstructure had ferrite and pearlite. This microstructure is commonly observed in low-carbon steels, thus reflecting the chemical composition shown in
Table 1. **Fig. 4** shows the SEM-BSE image of the pipe studied. The image shows that the microstructure exhibited well-defined ferrite and pearlite phases. The ferrite is the dominant phase. The study observed pores on the microstructure caused by pitting corrosion. The pitting pits may act as a crack initiation site, causing stress corrosion cracking (Fu et al., 2023).

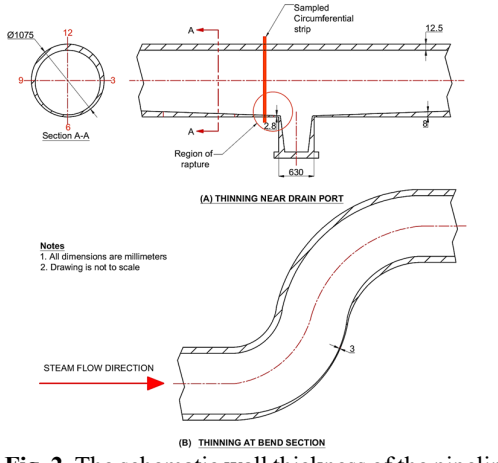


Fig. 2. The schematic wall thickness of the pipeline in cross-section and longitudinal directions.

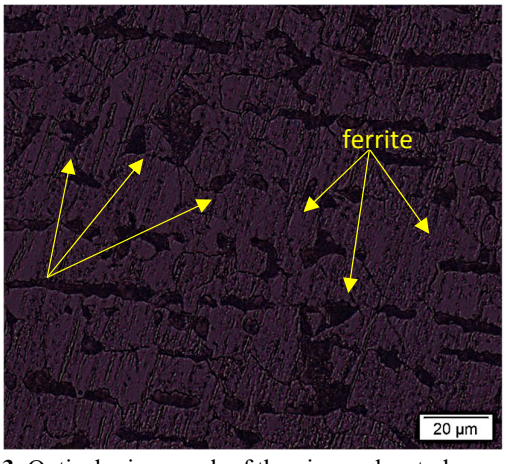


Fig. 3. Optical micrograph of the pipe under study.

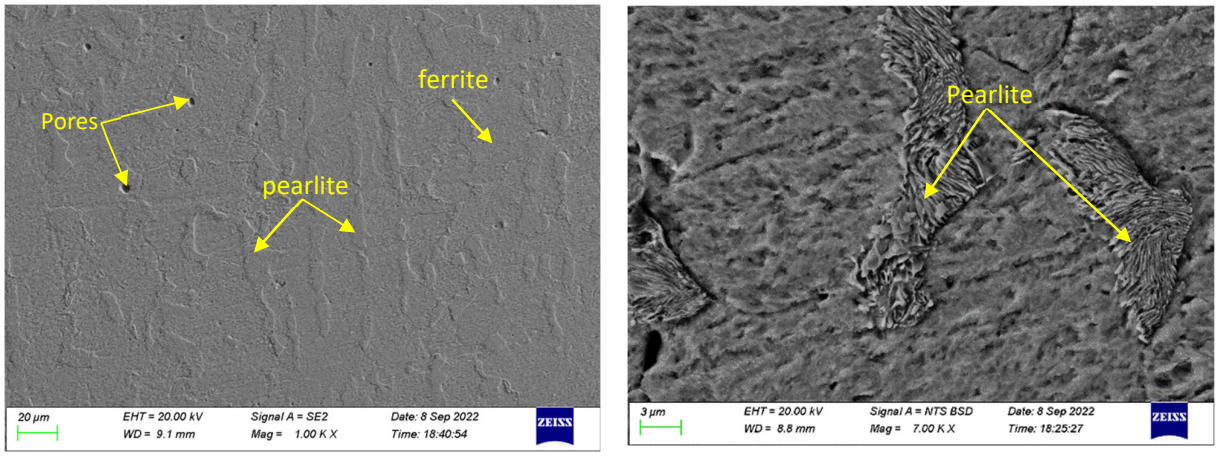
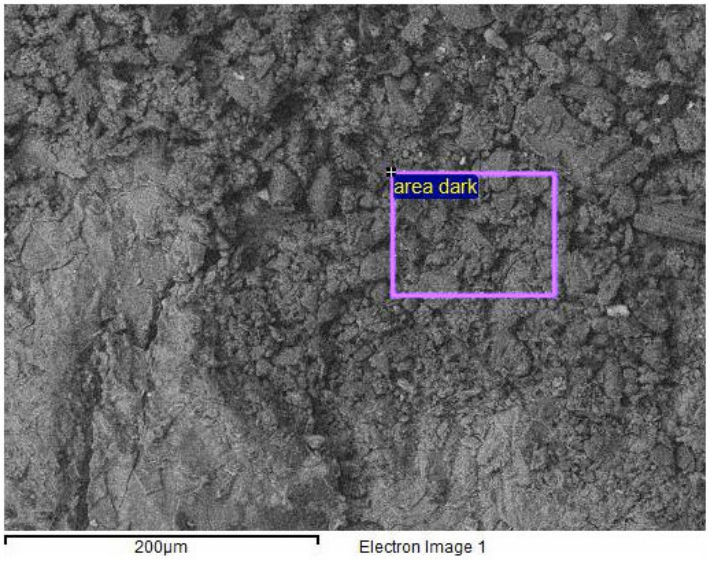
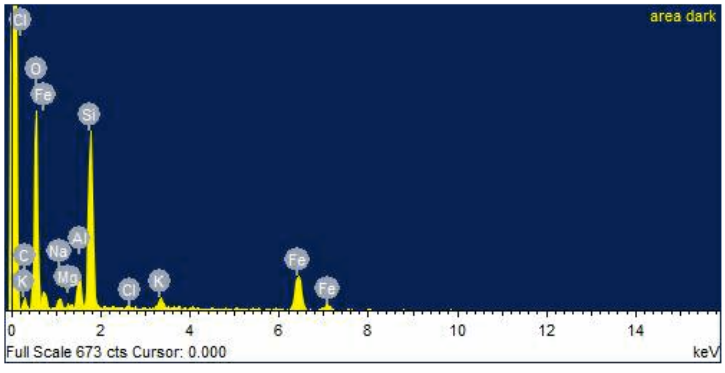


Fig. 4. SEM-BSE micrograph of the pipe under investigation.



(a)



(b)

Element	Weight%	Atomic%
C K	4.54	8.41
O K	43.66	60.76
Na K	1.51	1.46
Mg K	0.22	0.20
Al K	3.44	2.84
Si K	18.72	14.84
Cl K	0.14	0.09
K K	1.85	1.06
Fe K	25.92	10.33
Totals	100.00	

(c)

Fig. 5. SEM-BSE image and EDX of the steam pipeline surface.

3.2. Surface corrosion analysis

The SEM/EDX equipment studied the surface corrosion of the steam pipe. Table 3 shows the EDX analysis results. The results revealed the presence of elements mainly Fe, O, Si, Na, Cl, Mg, Al and K, as shown in **Fig. 5** and **Fig. 6**. The quantitative composition of the geothermal scale shows that amorphous silica was the main constituent in a few salts. Other

scales include iron silicate, calcium carbonate and sulphide. There are various mechanisms of silica scaling formation by precipitation through evaporation, flashing, and supersaturation of water droplets carried over from the production-well separators (Takayama et al., 2000).

With a drop in temperature or pressure in the surface pipework, the liquid fraction will flush or boil, causing supersaturation for silica that would end up in silica deposition (Opondo, 2005). Corrosion occurs due to contact between the silica and metal surface. Corrosion occurs due to contact between the silica and metal surface, thus influencing erosion-corrosion behaviour. The formed deposits have an amorphous or crystalline structure that can promote localised corrosion beneath the pipe (Opondo, 2005). Geothermal fluids such as hydrogen chloride, hydrogen sulfide, and silica cause multiple corrosion mechanisms and scaling (Royani et al., 2021). Sudden changes in flow velocities of particle-invested geothermal fluids occasionally result in tribo-corrosion. This corrosion behaviour results in material loss, thus damaging the surface layers. The corroded steam base metal undergoes mechanical failure due to the condensate-induced water hammer effect due to fluid flow. The mechanism of erosion-corrosion in low-carbon steel results in a rough surface. This surface texture is due to cyclic plastic deformation and smearing of the material (Brownlie et al., 2021). The impacting particles easily remove the smeared material from the pipe surface.

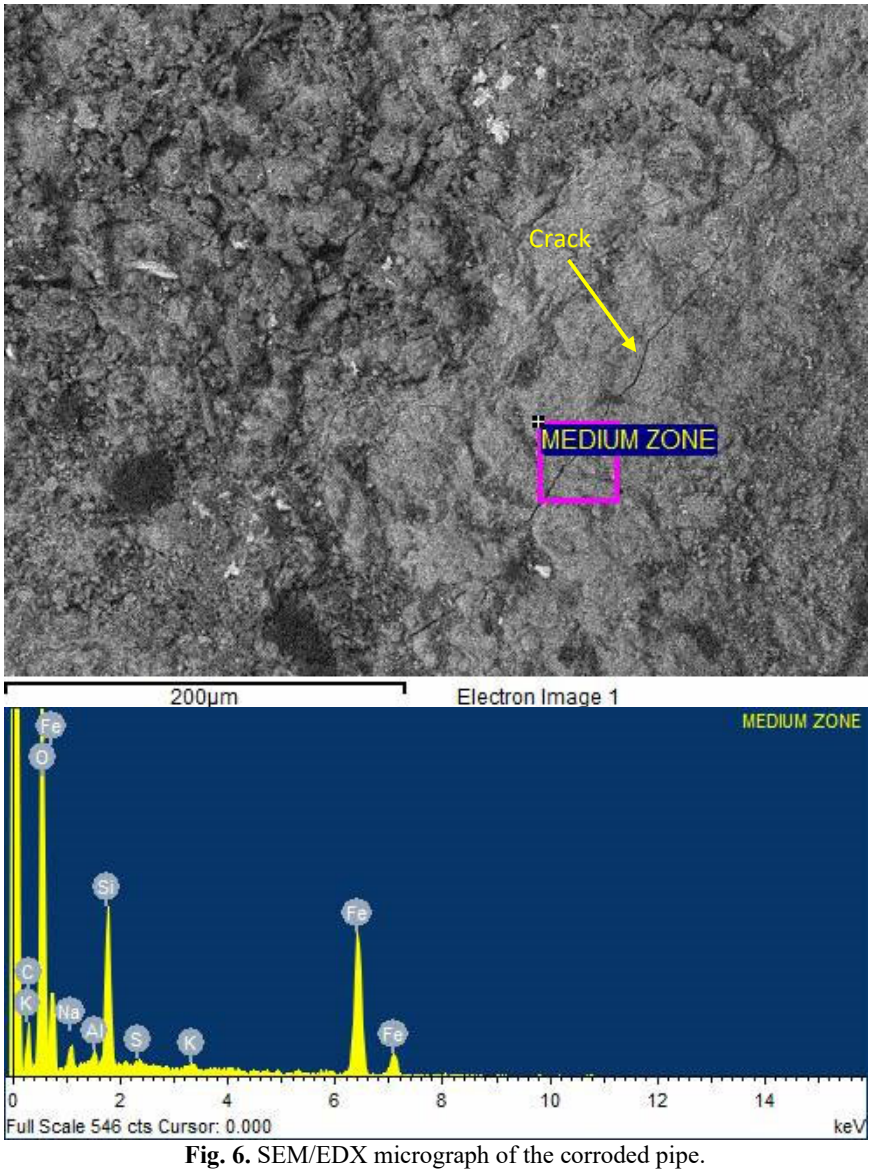


Fig. 6. SEM/EDX micrograph of the corroded pipe.

Table 3. EDX of corroded pipe.

Element	C	O	Na	Al	Si	S	K	Fe
Weight %	5.96	43.17	1.55	0.49	7.07	0.31	0.33	41.11
Atomic %	11.57	62.95	1.57	0.43	5.87	0.23	0.20	17.18

3.3. Findings and contributing factors

The study observed that the steam pipeline undergoes erosion-corrosion processes and metal deposits over time. Therefore, the steam pipeline failed due to corrosion damage resulting from erosion-corrosion. The deposits formed due to the chemical reaction between solid particles and steam with reactive agents such as hydrogen sulfide. Due to the fluid's low velocity, the solid particles and deposits cause erosion-corrosion at the particle and surface interface. The lower section of the steam pipe, especially at liquid discharge ports and pipe bends, experienced severe corrosion. The failure started gradually during the pipeline service and grew incrementally. The pipe wall thinning occurred due to the geothermal fluid/steam and pipe wall interaction. The study points out that the material selection for this application was not well-guided. Therefore, these sections of the steam pipeline require materials that are corrosive resistant with good creep strength. This approach will ensure the safety of the pipeline system and the operators and reduction in maintenance costs. The study also revealed that unprocedural maintenance procedures such as weld repair might have also accelerated corrosion activities.

The flow direction and velocity changes may cause the elbow to thin. This action significantly increases corrosion behaviour. For example, flow-accelerated corrosion occurs at the elbow and T-sections of the drain ports. The study observed that the tribocorrosion mechanism was the dominant corrosion mechanism. Hence, this mechanism damaged the surface layer and the base metal. This corrosion mechanism (erosion corrosion) in these steam pipelines caused localised thinning, thus causing weak sections. The scale of rupture of the pipeline material points towards a condensation-induced hammer near a drain port. Condensation occurs even for the insulated pipes due to heat transfer to the outside, but occasionally clogging or malfunctioning, allowing condensate to build up. The steam pressure, temperature and fluid velocities contribute to the intensity of hammer events. The generation of pressure waves occurs, causing the weakest section of the pipeline to rupture.

3.4. Possible mitigation measures

The following mitigation measures can be considered:

1. During material selection, corrosion resistance material should be considered for this application. The steam pipe should meet the minimum strength and corrosion requirement for service application in geothermal power plants.
2. Economically, the study recommends the use of corrosion-resistant steel to avoid repeated maintenance costs.
3. During operation, the study recommends that the pipeline system have steam traps. These traps will assist in the condensate removal whenever it forms. This design will ensure that the steam is dry.
4. Reduce the intensity of geothermal power plant metals' general corrosion by the inhibitory effect of surfactants and protective films on metal. The study also recommends coatings and linings for pipes above ground or underground.
5. The wall thickness at the affected areas, especially the lower side of the pipeline, all elbows and near the drain port, should have a higher thickness.
6. Routine checks of pipelines using ultrasonic waves will ensure proper monitoring of corrosion evolution in pipelines and the related wall thinning in the framework of maintenance operations.
7. Monitor and remove condensate periodically to keep the steam dry and maintain records to keep in check the trends of condensate formation and quantities.

3.5. Conclusion and recommendations

This study analysed a failure of a steam pipeline and made the following conclusions:

1. The steam pipeline failed due to erosion-corrosion caused by multiphase fluid containing solid particles and steam, causing thinning of the wall pipe. The chemical composition of the steel meets the standard High Strength Low alloy (HSLA) steel commonly used for oil and gas industries. The microstructure exhibited ferrite and pearlite.
2. The material used had low resistance to corrosion. The study recommends the application of creep-resistance steels at the drain port and elbows. However, joining dissimilar materials should be carefully done to avoid metallurgical changes at the weld joint.
3. The working fluid flow velocity, working pressure and temperature design procedures should be adhered to. There is a need to reduce the flow velocity and introduce steam purification agents. Hence, a reduction in erosion-corrosion activity.

References

Ávila, Á. M. D., De Oro, E. de J. H., Pérez, E. C. M., Núñez, E. E. N., & Unfried-Silgado, J. (2023). Evaluation of the Effect of Heat Input on Welded Joint Properties of ASTM A572 Grade 50 Steel Using the GMAW Process with 90Ar-10CO2 Shielding Gas and Spray Metal Transfer. *Soldagem e Inspecao*, *28*, 1–13. https://doi.org/10.1590/0104-9224/SI28.05

Brownlie, F., Hodgkiess, T., Pearson, A., & Galloway, A. M. (2021). A study on the erosion-corrosion behaviour of engineering materials used in the geothermal industry. *Wear*, *477*. https://doi.org/10.1016/j.wear.2021.203821

Carbos, T. R., Jorge, J. C. F., de Souza, L. F. G., de Souza Bott, I., & Mendes, M. C. (2020). Investigation into the Impact

Toughness of API 5L X80 Steel Weldments and its Relationship with Safe Welding Procedures. *Materials Research*, *23*(6). https://doi.org/10.1590/1980-5373-MR-2020-0363

Fu, Q., Qin, Q., Wei, B., Xu, J., Yu, C., & Sun, C. (2023). Stress corrosion cracking behavior of X80 pipeline steel under alternating current, Desulfovibrio desulfurican and cathodic protection potential. *Journal of Materials Research and Technology*, *24*, 7732–7744. https://doi.org/10.1016/j.jmrt.2023.05.055

Hu, M. J., Ji, L. K., Chi, Q., & Ma, Q. R. (2022). Microstructures and Fatigue Properties of High-Strength Low-Alloy Steel Prepared through Submerged-Arc Additive Manufacturing. *Materials*, *15*(23). https://doi.org/10.3390/ma15238610

Kusmono, & Khasani. (2017). Analysis of a failed pipe elbow in geothermal production facility. *Case Studies in Engineering Failure Analysis*, *9*(August), 71–77. https://doi.org/10.1016/j.csefa.2017.08.001

Liu, B., Yang, J., Du, C., Liu, Z., Wu, W., & Li, X. (2023). Stress corrosion cracking of X80 steel heat-affected zone in a near-neutral pH solution containing Bacillus cereus. *Npj Materials Degradation*, *7*(1), 1–15. https://doi.org/10.1038/s41529-023-00333-w

Opondo, K. M. (2005). Scale Deposition Experienced in Olkaria Well OW-34. *Proceedings World Geothermal Congress 2005*, *April*, 24–29.

Ribeiro, H. V., Reis Pereira Baptista, C. A., Fernandes Lima, M. S., Santos Torres, M. A., & Marcomini, J. B. (2021). Effect of laser welding heat input on fatigue crack growth and CTOD fracture toughness of HSLA steel joints. *Journal of Materials Research and Technology*, *11*, 801–810. https://doi.org/10.1016/j.jmrt.2021.01.038

Royani, A., Prifiharni, S., Priyotomo, G., & Sundjono, S. (2021). Corrosion Rate and Corrosion Behaviour Analysis of Carbon Steel Pipe At Constant Condensed Fluid. *Metallurgical and Materials Engineering*, *27*(4), 519–530. https://doi.org/10.30544/591

Sharma, S. K., & Maheshwari, S. (2017). A review on welding of high strength oil and gas pipeline steels. *Journal of Natural Gas Science and Engineering*, *38*, 203–217. https://doi.org/10.1016/j.jngse.2016.12.039

Takayama, K., Komiyama, N., Takahashi, Y., & Shakunaga, N. (2000). Silica Scale Abatement System. *Proceedings World Geothermal Congress 2000*, 3321–3326.

Villalobos, J. C., Del-Pozo, A., Campillo, B., Mayen, J., & Serna, S. (2018). Microalloyed steels through history until 2018: Review of chemical composition, processing and hydrogen service. In *Metals* (Vol. 8, Issue 5). https://doi.org/10.3390/met8050351

Wang, D., Xie, F., Wu, M., Sun, D., Li, X., & Ju, J. (2017). The effect of sulfate-reducing bacteria on hydrogen permeation of X80 steel under cathodic protection potential. *International Journal of Hydrogen Energy*, *42*(44), 27206–27213. https://doi.org/10.1016/j.ijhydene.2017.09.071



© 2025 by the authors; licensee Growing Science, Canada. This is an open access article distributed under the terms and conditions of the Creative Commons Attribution (CC-BY) license (http://creativecommons.org/licenses/by/4.0/).